Journal of ELECTRONIC MATERIALS, Vol. 45, No. 10, 2016
DOI: 10.1007/s11664-016-4761-5
© 2016 The Minerals, Metals & Materials Society

Structural and Optoelectrical Properties of ZnTe Thin Films Prepared by E-Beam Evaporation

REHANA ZIA,[1,4] FARHAT SALEEMI,[2] MADEEHA RIAZ,[1] and SHAHZAD NASSEM[3]

1.—Department of Physics, Lahore College for Women University, Lahore 54000, Pakistan. 2.—Govt. College for Women University, Sialkot, Pakistan. 3.—Centre for Solid State Physics, University of the Punjab, Lahore, Pakistan. 4.—e-mail: rzia1960@gmail.com

ZnTe thin films have been prepared by an electron-beam evaporation technique on glass substrates, changing the accelerating voltage and the substrate temperature at accelerating voltage of 2 kV. Structural analysis showed that all the films had cubic structure with preferential orientation along (111) direction, though (220) and (311) orientations were also present. The (111) peak intensity increased with increasing film thickness. The crystallite size increased with increasing film thickness. Conductivity measurements showed that the films were *p*-type. Films prepared at accelerating voltage of 2 kV exhibited minimum resistivity. Optical characterization indicated that both absorbing and transparent thin films can be achieved by using different deposition conditions. The optical bandgap value was found to vary with substrate temperature.

Key words: ZnTe, thin film, conductivity, optical bandgap

INTRODUCTION

II–VI semiconductors, due to their possible candidacy for formation of solar cells, light-emitting diodes (LEDs), and other optoelectronic devices, have gained importance over the past few decades. Compared with most other wide-bandgap II–VI compound semiconductors, which can be easily doped *n*-type, ZnTe, with a bandgap of 2.26 eV, shows *p*-type behavior. The dominant presence of any type of acceptor impurity and strong self-compensation effects prevent efficient *n*-type doping, which however would be suitable for ZnTe-based *p*–*n* junctions.[1]

Fabrication of low-resistance ohmic contacts on *p*-type CdTe is not easy, and better results have only been reported on low-resistivity material for photovoltaic converters.[2] The ohmic behavior of such contacts on high-resistivity materials such as ZnTe and CdTe has been found to depend strongly on reaction time. This leads to formation of polycrystalline *n*–i–*p* thin-film solar cells. The type of cell which incorporates wide-bandgap *n*-type CdS or $Zn_xCd_{1-x}S$ and *p*-type ZnTe semiconductors on opposite sides of high-resistivity (intrinsic) CdTe has many potential advantages compared with simple heterojunctions.[3] A small valence-band offset of 0.1 eV has been determined for the CdTe/ZnTe interface for thermally evaporated ZnTe, which is nearly ideal for charge transport, while highly *p*-doped ZnTe can be prepared by nitrogen incorporation,[4] both properties being necessary for good back contacts.[5]

ZnTe films can be developed by a number of techniques including molecular beam epitaxy, chemical vapor deposition, pulsed laser deposition, and vacuum evaporation to name but a few. Of these, vacuum evaporation has the advantage that large-area films can be grown. Desired film properties can be controlled by varying deposition conditions such as the accelerating voltage, substrate temperature, deposition rate, and film thickness.

We present the results of structural, optical, and electrical characterization of ZnTe thin films prepared by electron-beam evaporation under varying deposition conditions. The intention was to deposit

(Received February 4, 2016; accepted June 17, 2016; published online July 7, 2016)

Table I. Details of ZnTe films prepared by e-beam evaporation technique

Film	Accelerating voltage (kV)	Substrate temperature (°C)	Thickness nm ± 5% (nm)
#1	1	30	200
#2	2	30	200
#3	3	30	200
#4	2	100	200
#5	2	150	200
#6	2	200	200
#7	2	250	200
#8	2	300	200
#9	2	30	100
#10	2	30	150
#11	2	30	200
#12	2	30	250
#13	2	30	300

low-resistance *p*-type ZnTe films which, as interlayers, could improve the quality of back ohmic contacts on CdTe-based solar cells.

EXPERIMENTAL PROCEDURES

Preparation of ZnTe Thin Films

ZnTe thin films were grown by an electron-beam evaporation technique using an Edwards 306 coating unit. Soda-lime glass substrates were thoroughly washed in deionized water and degreased in an ultrasonic bath successively with acetone and isopropyl alcohol. After cleaning the deposition chamber with emery paper, cotton wetting with acetone, and drying using a dryer, approximately 150 mg source material, i.e., ZnTe (Merck, 99.99%), was placed in a molybdenum boat and glass slide and loaded into the chamber. The source shutter was used to start and stop the deposition process. When the vacuum in the chamber was better than 1×10^{-5} Torr, the source material was evaporated by applying approximately 13 mA high-tension current. The accelerating voltage was varied for various films. Film thickness was monitored using a quartz-crystal monitor. The deposited films were found to be stable with good adherence to the glass substrate. Film thickness was measured from transmission spectra.[6] The details of the prepared films are presented in Table I.

RESULTS AND DISCUSSION

Structural Properties

Structural analysis of the deposited films was performed using a Bruker D8 Discover x-ray diffractometer by the grazing-incidence x-ray diffraction (GIXRD) technique. Cu K_α radiation having λ = 1.5418 Å at 40 kV and 30 mA was used as x-ray source. Scanning was performed for 2θ values from 20° to 80°.

The x-ray diffraction patterns of thin films #10, #11, #12, and #13 (film thickness 150 nm to 300 nm) are reproduced in Fig. 1a–d, respectively. All films showed similar patterns. Comparing the observed peaks with Joint Committee on Powder Diffraction Standards (JCPDS) data revealed that the observed peaks corresponded to reflections from (111), (220), (311), and (421) planes, thus indicating the polycrystallinity of the films. The reflection from (111) direction dominated all spectra, but to varying extent. The lattice parameters were calculated using Bragg's relation

$$2d\,\sin\theta = n\lambda, \quad (1)$$

whereas the grain size was estimated using Scherrer's formula

$$D = \frac{k\lambda}{\beta\cos\theta}, \quad (2)$$

where k is a constant, β is the full-width at half-maximum (FWHM), λ is the wavelength of the x-rays used, and θ is the diffraction angle. Here, we used k = 1, λ = 1.5418 Å (wavelength of Cu K_α radiation), β as the FWHM of (111) peak, and a 2θ angle of 25.3° for the (111) diffraction peak to calculate the crystallite size. The full-width at half-maximum (FWHM) values for (111) peak were found to decrease from 1.2 for 150-nm-thick film to 0.35 for 300-nm-thick film, showing that the grain size increased with the film thickness. Table II provides a list of the crystallite size values calculated for films # 10, 11, 12, and 13, whereas the same is plotted in Fig. 2. The crystallite size was found to increase from 13 nm for 150-nm film to about 44 nm for 300-nm film. The grazing-incidence x-ray diffraction results indicate that the deposited ZnTe films showed good crystallinity. The reflection contribution from (111) plane was found to increase with layer thickness, as indicated in Fig. 1a–d.

The results of this study are in good agreement with results reported by many authors,[7–9] who also observed cubic structure for ZnTe films grown by various techniques and found reflection from (111) direction to dominate the diffraction spectrum, with minor reflections from (220) and (311) directions.

Fig. 1. XRD patterns of ZnTe thin film. (a) Film thickness = 150 nm, (b) film thickness = 200 nm, (c) film thickness = 250 nm, and (d) film thickness = 300 nm.

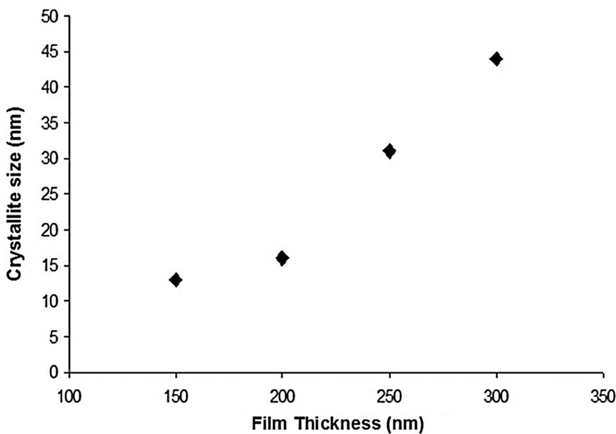

Fig. 2. Variation of crystallite size with ZnTe film thickness.

One study[10] determined the XRD patterns for ZnTe films of varying thickness grown by a thermal evaporation technique in the 2θ range from 20° to 60°, showing that the degree of preferred orientation and crystallite size were enhanced as the thickness was increased. They observed that the (111) peak intensity was related to the film thickness in the same manner as observed in this study.

Optical Properties

Measurement of the absorption spectrum is the most direct and perhaps simplest method for probing the band structure of a semiconductor. The fundamental absorption refers to excitation of an electron from the valence band to the conduction band. The magnitude of the absorption is expressed in terms of an absorption coefficient $\alpha(\lambda)$, which depends upon the wavelength of light. If a photon flux $\Gamma_0(\lambda)$ is present at $t = 0$ in the absorbing medium, then

$$\Gamma(\lambda, t) = \Gamma_0(\lambda)\exp[-\alpha(\lambda)t]. \quad (3)$$

The flux Γ is measured in units of photons $cm^{-2}\ s^{-1}$. The rate of free carrier generation $G\ (t)$ by intrinsic absorption is[11]

$$G(\lambda, t)\mathrm{d}t = -\mathrm{d}\Gamma(\lambda) = \alpha(\lambda)\Gamma(\lambda, t)\mathrm{d}t. \quad (4)$$

For all wavelengths relevant to solar cells, α is in the range from 10^3 cm^{-1} to 10^5 cm^{-1}.[12]

A Shimadzu recording UV-240 microprocessor-controlled double-beam spectrophotometer was used

Table II. Crystallite size as a function of film thickness

Film #	Thickness (nm) ± 5%	FWHM (radians)	Crystallite size (nm)
# 10	150	1.2	13
# 11	200	0.95	16
# 12	250	0.5	31
# 13	300	0.35	44

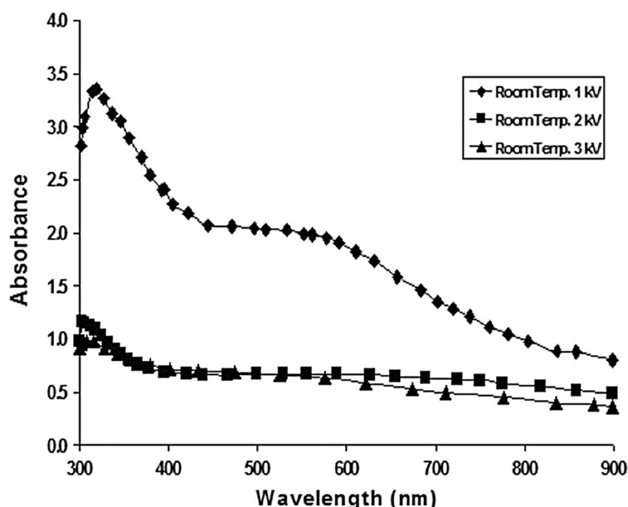

Fig. 3. Absorbance versus wavelength curves of ZnTe films grown at room temperature at different accelerating voltages.

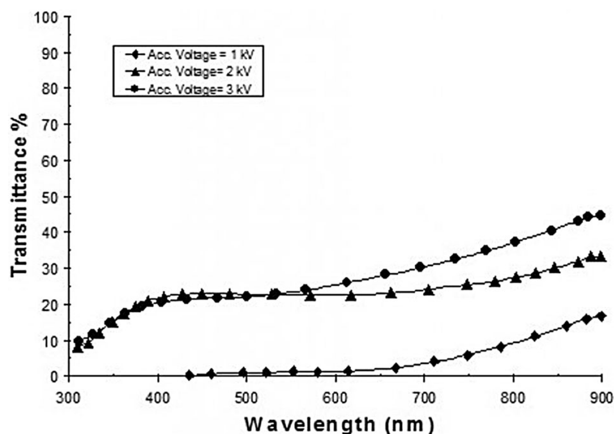

Fig. 4. Transmission versus wavelength curves of ZnTe films grown at various accelerating voltages.

to measure the optical transmittance of the prepared ZnTe thin films.*

The absorption and transmission spectra of ZnTe films grown at room temperature at accelerating

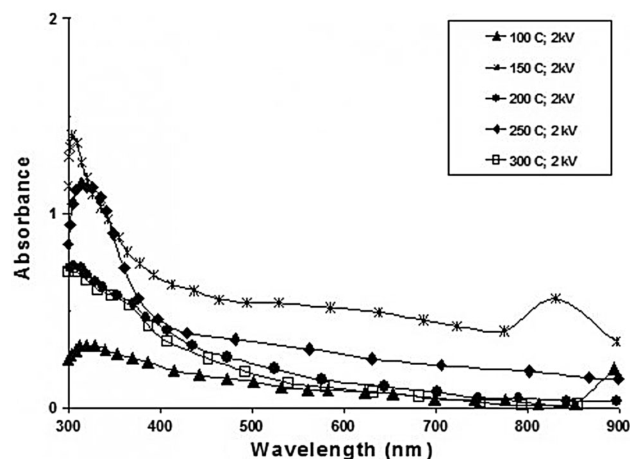

Fig. 5. Absorbance versus wavelength curves of ZnTe for films grown at different substrate temperature.

voltage varying from 1 kV to 3 kV were recorded (Figs. 3 and 4). It is seen that films grown at room temperature were highly absorbing, irrespective of the accelerating voltage. However, for films grown at elevated substrate temperature, absorption was low and transmission high; i.e., the films were nearly transparent, as shown in Figs. 5 and 6. In previous work,[13] both transparent and absorbing films were reported under different deposition conditions.

Transmittance and reflection curves of ZnTe thin films at room temperature were used to determine the bandgap energy by plotting the absorption coefficient versus photon energy. The relation between the transmission and reflection coefficients can be represented mathematically as

$$T = (1 - R)^2 \exp(-\alpha t)/1 - R^2 \exp(-2\alpha t), \qquad (5)$$

where the film thickness is represented as t. From the absorption coefficient α, the value of the optical bandgap (E_g) can then be calculated from the relation[14]

$$\alpha^2(h\upsilon) = A(h\upsilon - E_g). \qquad (6)$$

The values of α^2 were plotted as a function of $h\upsilon$, and the values of E_g were obtained by extrapolating the linear portion to the energy axis. Figure 7 shows a

*http://prr.hec.gov.pk/Thesis/363S.pdf.

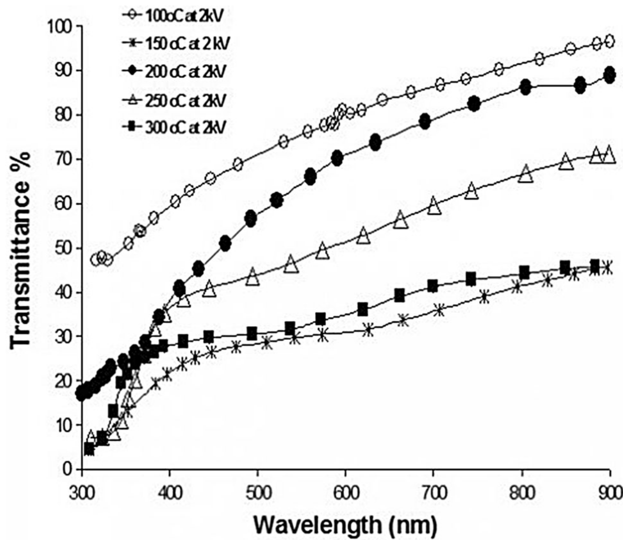

Fig. 6. Transmission versus wavelength curves of ZnTe films grown at various substrate temperatures.

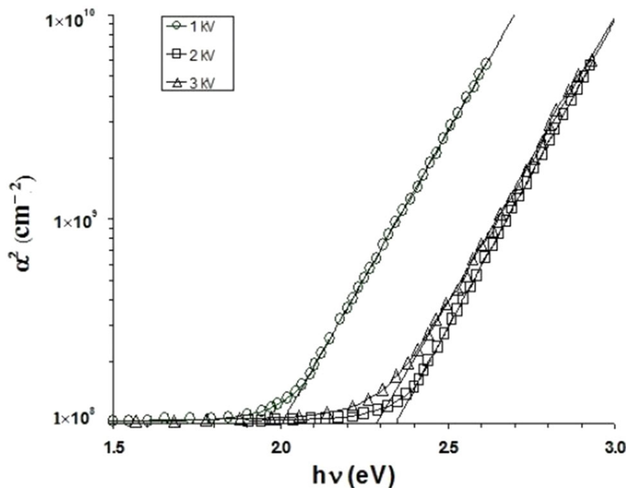

Fig. 7. α^2 versus $h\upsilon$ plot of ZnTe films grown at room temperature varying accelerating voltages.

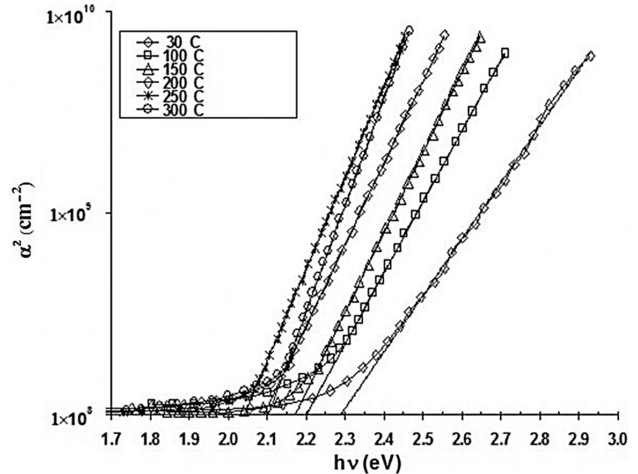

Fig. 8. α^2 versus $h\upsilon$ plot of ZnTe films grown at varying substrate temperatures at 2 kV accelerating voltage (film thickness 200 nm).

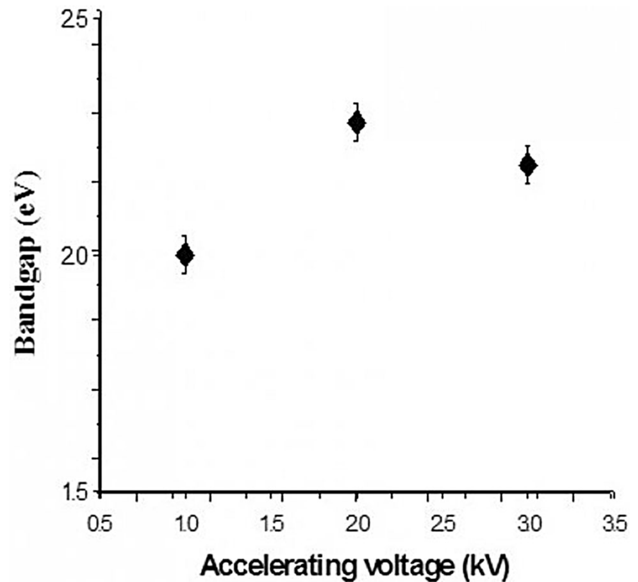

Fig. 9. Bandgap values of ZnTe thin films as a function of accelerating voltage.

plot of α^2 as a function of $h\upsilon$ for ZnTe thin films grown at room temperature for various accelerating voltages. Figure 8 shows a plot of α^2 versus $h\upsilon$ for films grown with substrate temperature varying from 30°C to 300°C. As is obvious from Fig. 9, the bandgap values for films grown at room temperature were slightly higher when the accelerating voltage was 2 kV as compared with films grown with accelerating voltage of 1 kV or 3 kV. Figure 10 shows a plot of the bandgap energy of ZnTe films as a function of substrate temperature. An inverse relationship between growth temperature (30°C to 300°C) and bandgap (2.28 eV to 2.05 eV) values can easily be observed. This trend may be explained by the fact that, as the substrate temperature was increased, the crystallite size increased. Other scientists have also reported similar inverse relationships between bandgap and substrate temperature values:[8,9] whereas one group[9] studied vacuum deposition of ZnTe in the temperature range of 303°C to 423°C and measured E_g variations from 2.3 eV to 2.02 eV, another group[8] observed E_g variations from 2.34 eV to 2.26 eV when the deposition temperature was varied from 30°C to 300°C during electron-beam evaporation of ZnTe thin films.

The results for E_g as a function of film thickness obtained in this study (Fig. 11) are in agreement with results reported by other studies,[9,15,16] where a decrease in bandgap with increasing film thickness

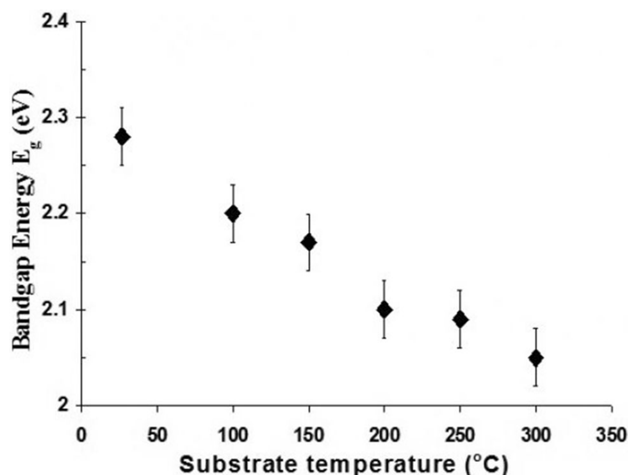

Fig. 10. Bandgap values of ZnTe thin films as a function of substrate temperature.

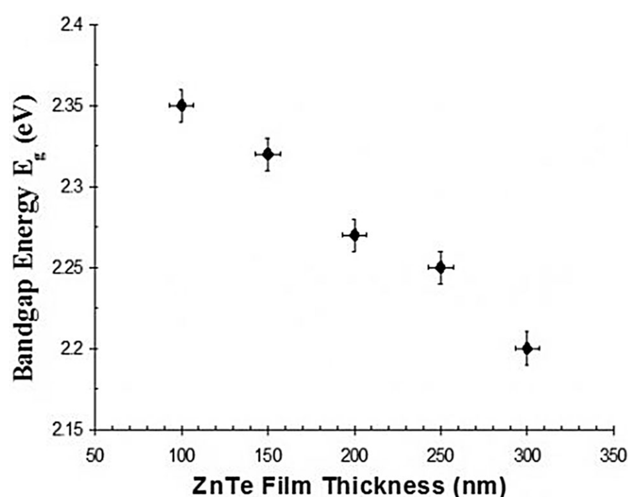

Fig. 11. Bandgap values of ZnTe thin films as a function of film thickness.

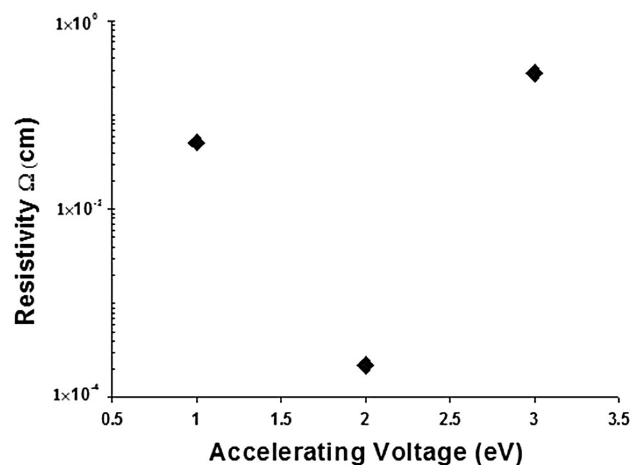

Fig. 12. Resistivity values of ZnTe thin films grown at different accelerating voltages.

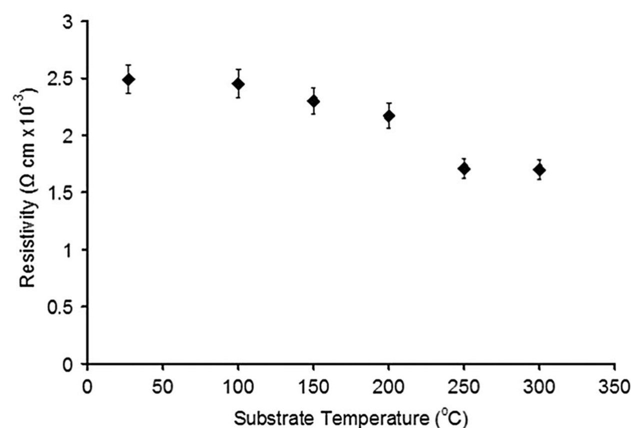

Fig. 13. ZnTe thin films resistivity as a function of substrate temperature at an accelerating voltage of 2 kV.

was also observed and related to increased density of localized states.

Electrical Properties

The ZnTe films prepared at fixed substrate temperature were electrically characterized using the van der Pauw method.[17] The resistivity values of films grown at room temperature as a function of accelerating voltage are shown in Fig. 12. These data show that the resistivity was minimum for films grown at 2 kV, being 2.19×10^{-4} Ω cm. The high values of resistivity measured at either side of 2 kV may be due to the fact that II–IV compounds conduct only due to deficiency of either of the elements. It is therefore speculated that, at lower accelerating voltage (1 kV), deficiency of Zn did not occur. Similarly, at 3 kV, the film was compensated, probably because of reevaporation of Te as well as Zn due to the raised temperature. One study[18] reported values of 3×10^{-3} Ω cm and 2×10^{-4} Ω cm for ZnTe films prepared by molecular beam epitaxy (MBE), whereas another[19] reported a high resistivity value (10^3 Ω cm) for ZnTe thin films prepared by the pulse laser deposition (PLD) method.

The resistivity values were also studied as a function of substrate temperature, as shown in Fig. 13. It is clear from Fig. 12 that the resistivity peaked at 100°C at about 2.45×10^{-3} Ω cm, then fell with increasing substrate temperature up to 300°C. This may once again be due to Zn deficiency. However, these values are higher than those at room temperature, because at higher temperature Te also reevaporates, thus compensating the ZnTe films.**

**http://prr.hec.gov.pk/Thesis/363S.pdf.

CONCLUSIONS

The results of the present study indicate that both absorbing and transmitting ZnTe thin films can be grown by the e-beam evaporation technique at different deposition conditions. The bandgap energy can be controlled by varying the film thickness and/or substrate temperature. Low-resistivity ZnTe thin films can be prepared by electron-beam-bombarded vacuum evaporation of ZnTe compound. Van der Pauw measurements showed that these films were *p*-type. Since these *p*-type ZnTe thin films showed a conduction mechanism due to Zn deficiency, the calculated resistivity value depended upon the deposition conditions. It was also seen that ZnTe thin film prepared at accelerating voltage of 2 kV exhibited the minimum resistivity. These films are found to be suitable for use as interlayers to improve the quality of back contacts in CdS/CdTe solar cells.

REFERENCES

1. G. Kudlek, N. Presser, J. Gutowski, K. Higerl, E. Avramof, A. Pesek, H. Pauli, and H. Sitter, *J. Cryst. Growth* 138, 81 (1994).
2. R.H. Bube, *Solar Cells* 23, 1 (1988).
3. D. Riovx, D.W. Niles, and H. Hochst, *J. Appl. Phys.* 73, 8381 (1993).
4. T. Baron, K. Saminadayar, and N. Magrea, *J. Appl. Phys.* 83, 1354 (1998).
5. B. Spath, J. Fritsche, F. Sauberlich, A. Klein, and W. Jaegermann, *Thin Solid Films* 480, 204 (2005).
6. J.C. Manifacier, J. Gasiot, and J.P. Fillard, *J. Phys.* 9, 1002 (1976).
7. J. Pattar, S.N. Sawant, M. Nagaraja, K.M. Balakrishna, G. Sanjeev, and H.M. Mahesh, *Int. J. Electrochem. Sci.* 4, 369 (2009).
8. N. Pradhan and X.G. Peng, *J. Am. Chem. Soc.* 129, 3339 (2007).
9. R. Amutha, A. Subbarayan, and R. Sathyamoorthy, *Cryst. Res. Technol.* 41, 1174 (2006).
10. A.A. Ibrahim, N.Z. El-Sayed, M.A. Kaid, and A. Ashour, *Vacuum* 75, 189 (2004).
11. J.I. Pankove, *Optical Processes in Semiconductors* (New York: Dover, 1980).
12. A.L. Fahrenbruch and R.H. Bube, *Fundamentals of Solar Cells* (London: Academic, 1985).
13. T. Baron, K. Saminadayar, and N. Magrea, *J. Appl. Phys.* 83, 1354 (1998).
14. A. Barlev, *Semiconductor and Electronic Devices*, 3rd ed. (New York: Prentice Hall, 1992).
15. G.I. Rusu, P. Pupelita, N. Apetroari, and G. Popa, *J. Optoelectron. Adv. Mater.* 7, 829 (2005).
16. M.S. Hossain, R. Islam, and K.A. Khan, *Chalcogenide Lett.* 7, 21 (2010).
17. L.J. Van der Pauw, *Philips Res. Rep.* 13, 1 (1958).
18. T. Ohtsuka, M. Yoshimura, K. Morita, and M. Koyama, *Appl. Phys. Lett.* 67, 9 (1995).
19. B. Kotlyarchuk and V. Savchuk, *Phys. Status Solidi B* 244, 1714 (2007).